Geophysical Research Letters

Key Points:
- A new Deep Argo pilot array improves spatial and temporal resolution of bottom water sampling in the Australian Antarctic Basin
- The floats capture the return of high salinity Ross Sea Bottom Water to the region after a period of multi-decadal freshening
- A simple Optimum Multiparameter calculation quantifies the local zonal variation in the new water mass concentrations from 2018 to 2020

Supporting Information:
- Supporting Information S1
- Table S1

Correspondence to:
S. G. Purkey,
spurkey@ucsd.edu

Spatial Variability of Antarctic Bottom Water in the Australian Antarctic Basin From 2018–2020 Captured by Deep Argo

George Thomas[1], Sarah G. Purkey[1], Dean Roemmich[1], Annie Foppert[2,3,4], and Stephen R. Rintoul[2,3,4]

[1]Scripps Institution of Oceanography, UCSD, San Diego, CA, USA, [2]CSIRO Oceans and Atmosphere, Hobart, Tasmania, Australia, [3]Centre for Southern Hemisphere Oceans Research, Hobart, Tasmania, Australia, [4]Australian Antarctic Program Partnership, Hobart, Tasmania, Australia

Abstract There are two varieties of Antarctic Bottom Water present in the Australian Antarctic Basin (AAB): locally produced Adélie Land Bottom Water (ALBW) and distantly produced Ross Sea Bottom Water (RSBW). Between 2014 and 2018, RSBW has rebounded from a multidecade freshening trend. The return of the salty RSBW to the AAB is revealed by six Deep Argo floats that have occupied the region from January of 2018 to March of 2020. The floats depict a zonal variation in temperature and salinity in the bottom waters of the AAB, driven by the inflow of RSBW. A simple Optimum Multiparameter Analysis based on potential temperature and salinity gives a sense of scale to the composition of the bottom waters, which are nearly 80% of the new, salty RSBW in the south-east corner of the basin by 2019 and generally less than 40% to the west closer to the ALBW outflow region and the abyssal plain.

Plain Language Summary The dense waters that form along the Antarctic coast and fill the global deep oceans have been warming and freshening over the past three decades. This water is integral to the earth's natural system of temperature regulation. New robotic floats from the Deep Argo program are able to record temperature, salinity, and pressure down to the bottom of the ocean and are capturing variability in the quantity and properties of these dense waters near their formation sites better than ever before. Here we examine data from the first 2 years of float deployments in the Indian sector of the Southern Ocean to quantify the rebound in salinity of dense water from the Ross Sea and study how different varieties of this dense water spread and fill the Australian Antarctic Basin before ultimately flowing out into the Indian and Pacific Oceans.

1. Introduction

Over the past three decades Antarctic Bottom Water (AABW) has played a crucial role in mitigating the increase of anthropogenic atmospheric warming through the sequestration of heat into the abyssal (greater than 4,000 m depth) ocean. Decadal occupations of hydrographic sections gridding the deep ocean conducted by the Global Ocean Ship-based Hydrographic Investigations Program (GO-SHIP; Talley et al., 2016) have shown that the abyssal ocean has warmed significantly throughout the globe (Desbruyères et al., 2016; Fukasawa et al., 2004; Kawano et al., 2006; Kouketsu et al., 2011; Purkey & Johnson, 2010). This deep warming is likely driven by changes in the salinity of the dense shelf waters around Antarctica that produce AABW (e.g., Aoki et al., 2005, 2013; Kobayashi, 2018; Menezes et al., 2017; Purkey & Johnson, 2012, 2013; Rintoul, 2007; Shimada et al., 2012; van Wijk & Rintoul, 2014), which have undergone short- and long-term variability owing to increased glacial runoff and interannual variability in sea ice production and export (Castagno et al., 2019; Jacobs et al., 2002; Jacobs & Giulivi, 2010; Silvano et al., 2020). Furthermore, high resolution models have shown a similar climate signal of abyssal warming, driven by a combination of decreased AABW production from anthropogenic freshening and warming on the shelves near Antarctica and from warmer waters being advected through the bottom limb of the MOC (Boé et al., 2009; Bryan et al., 2014; Newsom et al., 2016). Most recently, a long-term freshening trend on the Ross Shelf, one of the primary formation regions of AABW, reversed in 2014 (Castagno et al., 2019; Silvano et al., 2020). Here, we use the new Deep Argo data in 2018–2020 to show the rebound in high salinity shelf water is detectable in the AABW in the eastern portion of the Australian Antarctic Basin (AAB).

AABW forms in distinct regions on the Antarctic coast (Orsi et al., 1999) that possess certain shelf conditions, including large coastal polynyas, brine rejection due to creation of sea ice, and strong air-sea interaction (e.g., Williams et al., 2008). In each region, bottom water originates from dense shelf water (DSW) sinking down the continental slope and entraining local water masses. The various sources of AABW supply the dense water masses that sink and ventilate the deep ocean basins worldwide (e.g., Johnson, 2008; Rintoul, 1998). There they feed the bottom limb of the Meridional Overturning Circulation (MOC; Ganachaud & Wunsch, 2000; Lumpkin & Speer, 2007; Sloyan & Rintoul, 2001; Talley, 2003) and fill the bottom half of the global ocean (Johnson, 2008).

Two recurrent areas of AABW formation are the Adélie and George V Land (AGVL) coast and the Ross Sea, both of which supply bottom water to the AAB (Rintoul, 1998, 2007; van Wijk & Rintoul, 2014; Williams et al., 2010) before mixing in the Antarctic Circumpolar Current (ACC) and eventually being exported into the Indian and Pacific Oceans. Each region produces bottom water with unique characteristics and as such are named Adélie Land Bottom Water (ALBW) and Ross Sea Bottom Water (RSBW). RSBW and ALBW temperature and salinity properties are distinct, owing to differences in the production processes of the two water masses. The RSBW production regime is mostly governed by a wide continental shelf and a land boundary that limits westward outflow of shelf water, while its salinity is increased by brine rejection processes. This historically produces the saltiest variety of AABW, which flows out of the western side of the Ross Sea, around Cape Adare, and into the AAB (Gordon et al., 2004, 2009, 2015; van Wijk & Rintoul, 2014). Conversely, because the ALBW formation region lacks these properties, it relies on heavy brine rejection in a coastal polynya over the Adélie Depression, which is located in the lee of the Mertz Glacier Tongue (Figure 1; Aoki et al., 2017; Bindoff, Rintoul, et al., 2000; Bindoff, Rosenberg, et al., 2000; Rintoul, 1998; Williams et al., 2008). Maintenance of this polynya is likely aided by the strength of katabatic winds (Wendler et al., 1997), atmospheric forced variability in surface winter temperatures and wind fields (Campagne et al., 2015; Marsland et al., 2007; Massom et al., 2001), and rates of Modified Circumpolar Deep Water (MCDW) intrusion (Aoki et al., 2013; Williams et al., 2008).

Observations within and near formation regions have shown large variations in the properties of RSBW and ALBW since the 1960s (Figure 2a; e.g., Aoki et al., 2005; Jacobs & Giulivi, 2010; Rintoul, 2007; Swift & Orsi, 2012; van Wijk & Rintoul, 2014). The calving of the Mertz Glacier Tongue in 2010 altered ALBW composition on an interannual time scale, owing to changes in factors such as sea ice production (Snow et al., 2018; Tamura et al., 2016) and input of freshwater from continental melt (Aoki et al., 2013, 2017; Kobayashi, 2018) and sea ice (Shadwick et al., 2013). High Salinity Shelf Water (HSSW) in the Ross Sea, a precursor to RSBW, freshened at a rate near 0.03 dec^{-1} between the 1960s and 2000s (Jacobs et al., 2002; Jacobs & Giulivi, 2010) but rebounded very quickly in the period 2014–2018 (Castagno et al., 2019). The rebound in HSSW is closely correlated to an increase in the local sea ice formation, triggered by anomalous winds between 2015 and 2018 (Silvano et al., 2020), overcompensating for the multidecadal freshening trend driven by an increase in glacial melt water to the region (Jacobs et al., 2002; Jacobs & Giulivi, 2010). The fresher shelf water prior to 2014 created a fresher variety of RSBW and affected the quantity, circulation, and properties found along the outflow path of RSBW and ALBW, which was observed as a deep freshening or warming on abyssal pressure surfaces throughout the Indo-Pacific Southern Ocean and as far north as the Southwest Pacific Basin (Aoki et al., 2005; Johnson, 2008; Menezes et al., 2017; Purkey et al., 2019; Rintoul, 2007; Shimada et al., 2012; Swift & Orsi, 2012; van Wijk & Rintoul, 2014). Following the rebound in the salinity of RSSW, the salinity of RSBW increased in 2018/2019, reversing the multidecadal freshening trend (Silvano et al., 2020).

Despite variability in production of this deep, cold water being a significant element of the earth's global anthropogenic warming budget, in situ observations of this annual cycle are relatively sparse, with the majority of data used to study the region concentrated in the austral summer months due to problems posed by wintertime ship observations (Purkey & Johnson, 2010). Beginning in 2014, the international oceanic observation program Argo began deploying autonomous Deep Argo floats capable of sampling temperature, salinity, and pressure down to a depth of 6,000 m. This relatively new Deep Argo Program represents a significant step toward tracking changes in the abyssal ocean, since Core Argo floats are only capable of profiling down to 2,000 m (Roemmich, Alford, et al., 2019). With growing critical mass, data from these floats will provide far greater spatial and temporal resolution of abyssal processes than was previously possible from repeat hydrographic GO-SHIP sections (Johnson et al., 2019; Kobayashi, 2018; Roemmich, Sherman, et al., 2019).
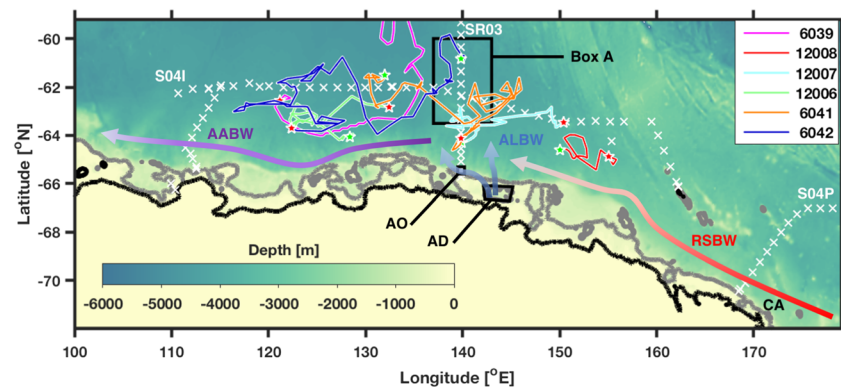
Figure 1. Paths of six Deep Argo floats (colored lines) are shown in relation to bathymetry from ETOPO1 (color bar; https://doi.org/10.7289/V5C8276M). The deployment position for each float is marked by a green star, and the most recent profile position as of 1 April 2020 is marked by a red star. CTD profile locations from the most recent occupations of the three previously mentioned GO-SHIP sections are marked by white x's and labeled. Additionally, the 0 and 500 m depth isobaths (thick black and gray lines, respectively) and locations such as the ALBW outflow (AO) region, Adélie depression (AD), and cape Adare (CA) are shown. Box A, used in Figure 2a, is also shown. Finally, general flow paths of Adélie Land Bottom Water (ALBW), Ross Sea Bottom Water (RSBW), and the mix of the two here referred to simply as Antarctic Bottom Water (AABW), in the region are represented by blue, red, and purple arrows, respectively.

Here we describe the properties and sources of AABW found in the southern AAB and quantify the return of salty RSBW spreading into the AAB from the east, as observed by Deep Argo floats from January of 2018 to March of 2020. Furthermore, we assess the viability of Deep Argo in such a hostile region and demonstrate the value these data provide. In the next section, we will describe the Deep Argo and GO-SHIP data, as well as the analysis methods we used to produce our results. These results will be presented in section 3, and in section 4 we will discuss and explore their meaning.

2. Data and Methods

Between January 2018 and March 2019, eight Deep SOLO floats were deployed in the AAB with the purpose of providing a preliminary look at AABW production in this region (supporting information Table S1; Figure 1). The Deep SOLOs, one of the four models of Deep Argo floats, profile from the surface to within 3 m of the bottom or to a maximum pressure of 6,000 dbar, measuring temperature, salinity, and pressure at user-prescribed intervals between the sea surface and bottom (Roemmich, Sherman, et al., 2019). The Deep SOLOs are outfitted with a wire for a passive bottom detection as well as an ice sensing algorithm (Klatt et al., 2007; Roemmich, Sherman, et al., 2019). Five floats fabricated by Scripps Institution of Oceanography (SIO) were deployed in January–February of 2018 from the *R/V Investigator*. Three additional Deep SOLO floats, provided by the Commonwealth Scientific and Industrial Research Organization (CSIRO) and built by SIO's commercial partner MRV Systems, were deployed in January–March of 2019 from the *R/V Kaiyo Maru* (Table S1; Figure 1). The six floats nearest the continental shelf are the focus of this paper (Figure 1).

All Deep SOLO floats carry Seabird SBE-61 CTD (conductivity, temperature, depth) sensors, with accuracy goals of $\pm0.001°C$, ±0.002, and ±3 dbar for temperature, salinity and pressure, respectively. All Deep Argo data were obtained from the Argo Global Data Assembly Center (GDAC) on 1 April 2020 (https://doi.org/10.17882/42182). The only correction for the conductivity cell compressibility coefficient (cpcor) is applied to all floats from the default value of -9.57×10^{-8} dbar^{-1} to -11.66×10^{-8} dbar^{-1} following Murphy and Martini (2018; Roemmich, Sherman, et al., 2019) since DMQC adjustments, including this correction, had not yet been applied to the adjusted salinity field in the GDAC at the time the data were downloaded. In addition, any salinity spikes (defined as a change greater than 0.01 between sampling bins) were removed, including very fresh spikes found in the bottom 1–2 bins of some profiles, possibly owing to low conductivity driven by increased sediment close to the bottom. Potential temperature (θ) and depth are derived from the CTD profile. In addition, we calculate potential density (σ_4) for the temperature-salinity range observed in the region at 4,000 dbar for reference.
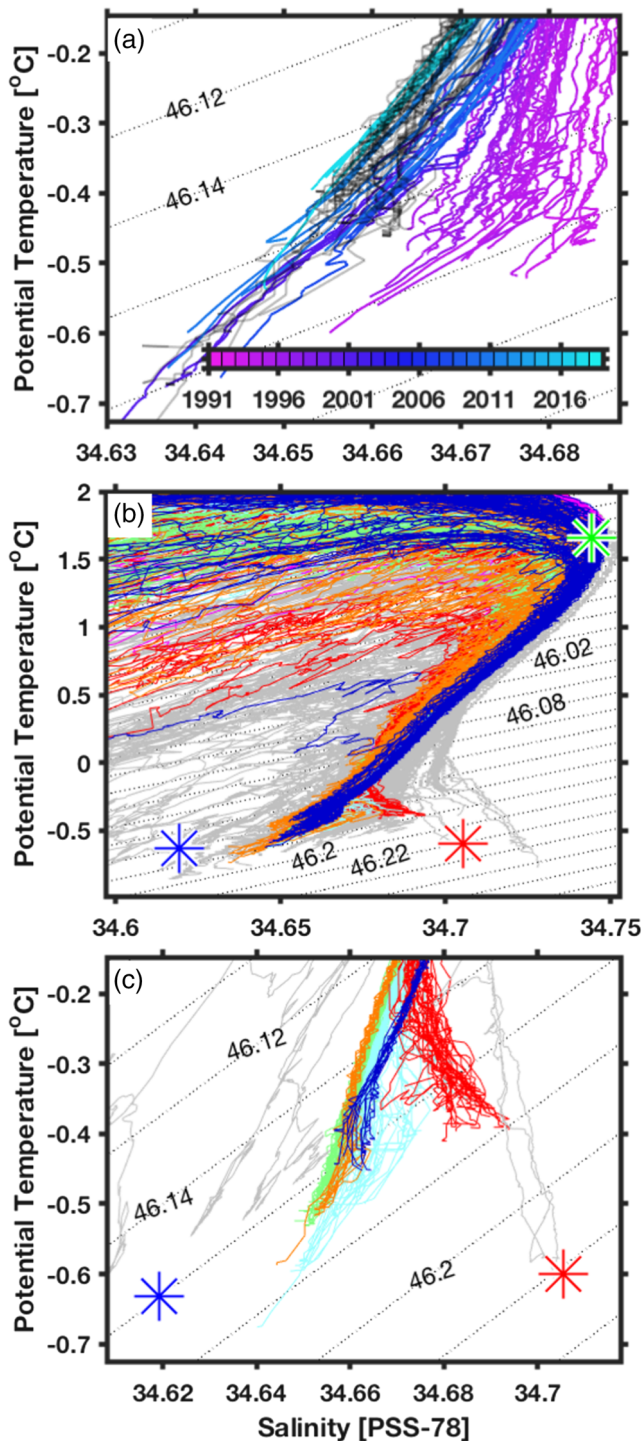
Figure 2. (a) θ-S profiles from all occupations (color bar) of SR03 and S04I within Box A (Figure 1) with float profiles (dark gray) from the region. (b) All float profiles (see Figure 1 color legend) with all years of the GO-SHIP CTD profiles shown in Figure 1 (gray). (c) A zoomed in view of (b), showing only profiles of floats 12006, 12007, 12008, cycles 19–30 (May-September 2018) of float 6042, and cycles 261–276 (December 2018-February 2019) of float 6041 (Table S1). Subplots show σ_4 contours (black dotted) and the RSBW, ALBW, and CDW endmembers represented by red, blue, and green asterisks, respectively.

No floats had a detectable drift in salinity. Using all profiles taken in water deeper than 3,000 m where the θ-salinity relationship is relatively tight away from the continental slope, all floats show a scatter within ±0.004 of the mean salinity along the 0.5°C potential isotherm with time, with most falling within the accuracy goal of ±0.002 over the time considered here. In addition, all float and colocated GO-SHIP salinity profiles within 220 km agreed within the ±0.002 in the potential isotherm range between 0 and 1°C.

Due to the lack of location data for winter profiles taken under sea ice, the locations of more than a quarter of the total float profiles are unknown (Table S1). Using maximum recorded depth as a constraint, we have developed a novel, simple method of determining revised float paths (supporting information). In order to serve as an example, only the winter 2018 profiles of float 6042 were altered (Figure S1).

Multiple occupations of high quality, full depth, ship-based CTD profiles collected along three GO-SHIP hydrographic track lines (https://cchdo. ucsd.edu/) are also considered here, including SR03, a meridional line along 140°E, occupied 10 times between 1991 and 2018, S04I, a zonal line along 62°S, occupied three times between 1995 and 2013, and S04P, which starts along the continental shelf near Cape Adare and heads northeast before following latitude 67°S, occupied three times between 1992 and 2018 (Figure 1). All GO-SHIP sections provide high quality CTD data measured on decadal timescales along set paths throughout the ocean. Vertical sections are measured to within 10–20 m of the bottom. The CTD salinity data are all calibrated to bottle salinities that are referenced to the International Association for the Physical Sciences of the Oceans (IAPSO) standard seawater. The shipboard CTD sensor has accuracies of ±0.002 for salinity, ±0.002°C for temperature, and ±3 dbar for pressure (Joyce, 1991). Only data with good quality control flags were used. We apply a 20 dbar half width vertical Hanning filter to all GO-SHIP CTD profiles.

To provide an estimate of the fraction of the recent, salty variety of RSBW present in the region, a simple version of an Optimum Multiparameter (OMP) analysis was performed, based solely on two conservative tracers: θ and salinity (Tomczak & Large, 1989). An OMP analysis uses a system of linear equations to determine what fraction of different water masses are present. For the purposes of this paper, it serves as a back-of-the-envelope calculation to determine the distribution of ALBW versus the new, salty RSBW along the bottom of the near-shelf AAB. A system of three linear equations with a nonnegative constraint was solved at each depth of each profile (Equation 1).

$$x_1\theta_{ALBW} + x_2\theta_{RSBW} + x_3\theta_{CDW} = \theta_{obs} \tag{1a}$$

$$x_1 S_{ALBW} + x_2 S_{RSBW} + x_3 S_{CDW} = S_{obs} \tag{1b}$$

$$x_1 + x_2 + x_3 = 1 \tag{1c}$$

Equations 1a and 1b conserve potential temperature (θ) and salinity (S) and Equation 1c conserves mass. The fraction of ALBW, RSBW, and CDW for each in situ observation (obs) of θ and S is given by x_1, x_2, and x_3, respectively. It is important to note that since two of our end members are similar in temperature, the fraction of ALBW versus RSBW is mostly determined by Equation 1b and is equivalent to looking at the fractional change in salinity.

The ALBW, RSBW, and CDW endmember temperatures and salinities (Equations 1a and 1b, $\theta/S_{ALBW,RSBW,CDW}$) are estimated from 2018 GO-SHIP cruises (Table S2). The RSBW endmember (Table S2; Figures 2b and 2c; red asterisk) properties of 34.704 and −0.599°C are taken to be the average of the bottom properties at the three southernmost positions of the 2018 S04P occupation that are not on the continental slope (Figure 2b, gray). These profiles are roughly between 69.6 and 70.2°S, with a maximum depth range of ~2,700 to ~2,800 m (Figure 1). These profiles were chosen because they display a clear RSBW signature along the bottom. Note that here we are choosing the RSBW endmember to be RSBW in 2018, representing the recent post-2014 shift toward salty RSBW. Therefore, any fraction of RSBW discussed hereafter represents the fraction of post-2014 RSBW. The ALBW endmember (Table S2; Figures 2b and 2c; blue asterisk) properties of 34.619 and −0.632°C are taken to be the average of the bottom values from the four SR03 profiles, sampled in 2018, within the ALBW outflow region, which we have defined to be the continental slope between 65.3 and 65.6°S. The maximum depth of these profiles ranges from ~800 to ~2,400 m and shows a large range in θ-S, but the mean properties are consistent with previous studies (Snow et al., 2018). The southernmost profile was excluded because it only extends to a depth of less than 300 m. The CDW endmember (Table S2; Figure 2b; green asterisk) properties of 34.733 and 1.831°C were defined from the position in θ-S space of the salinity maximum.

3. Results

The six Deep Argo floats measured the spatial distribution of bottom properties in the southeastern AAB, providing insight into the general flow paths of ALBW and RSBW into the region (Figure 1; blue and red arrows, respectively). The floats spanned a zonal distance of roughly 2,300 km between 115 and 160°E and between 60°S and the Antarctic continental slope (Figure 1). There was no significant pattern of zonal movement, with three floats drifting east-to-west and three flowing west-to-east. Float parking depth mostly ranged from 0 to 600 dbar off the bottom, except for floats 12006 and 12007, which mostly parked at a set pressure of 2,500 to 3,000 dbar regardless of bottom depth during the study period. During the winter and spring of 2018, floats 6041 and 6042 were under ice from August to November. In the winter and spring of 2019, the floats disappeared under ice any time from May–July and returned in December or January.

Observations between 1991 and 2018 from shipboard CTD measurements along GO-SHIP tracks SR03 and S04I show the temporal variability in bottom properties observed in recent decades over the abyssal plain and on the continental slope (Figure 2a). This variability reflects changes in both local varieties of AABW and is consistent with previous findings (e.g., Aoki et al., 2005, 2013; Johnson, 2008; Roemmich, Sherman, et al., 2019).

The southern end of SR03 between 60 and 64.5°S is located downstream from the ALBW formation region and shows the variations in both ALBW and RSBW between 1991 and 2018 (Figure 2a). Here, RSBW sits above ALBW and is seen as a salty kink, or a bend, in the θ-S curve around −0.45°C in most years (Figure 1, Box A; Figure 2a). Along −0.4°C, a gradual progression toward fresher conditions is observed, freshening from 34.68 in 1991 to 34.65 in 2011, consistent with the arrival of RSBW from the 1980s–2010s traveling west from the Ross shelf to 140°E. The 2018 SR03 occupation reveals a slight rebound of 0.01, indicating that the salty RSBW that began in 2014 (Castagno et al., 2019) has reached 140°E (Figure 2a).

The Deep Argo float data map the spatial extent of the return of higher salinity RSBW in the basin in 2018/2019 (Figures 2c and 3). The easternmost float, located in the southeast corner of the basin at ~150°E, captured the youngest RSBW in the basin that flows in from the east around Cape Adare (Figure 1; float 12008, red). Consistent with Silvano et al., 2020, the February 2018 occupation of the 150°E line showed that the deep waters here had warmed by 0.1°C and increased in salinity by 0.03 since the last occupation in 2011. The float data in 2019 also show the densest water between 46.16 and 46.18 kg/m^3 σ_4 have increased salinity by 0.04 compared to the 2011 hydrographic data, a rebound not seen in waters of similar density at the western end of the basin (Figure 2c; float 12008, red). The furthest east profile at 155.8°E is coincidental in θ-S space with profiles measured along S04P in 2018 (Figure 2(c); gray) at 46.18 kg/m^3, and it is as salty as bottom water found in the basin in 1991. The OMP analysis supports a strong presence of RSBW in the profiles of 12008, indicating that it is composed of up to 80% RSBW (Figure 3a).

The presence and fraction of new salty RSBW in the study area have a large zonal variation. In the more central floats (Figure 2c; such as float 12007, light blue, and float 6041, orange), the salty kink that indicates the presence of new, salty RSBW appears slightly higher in the water column, displaced off the bottom by the
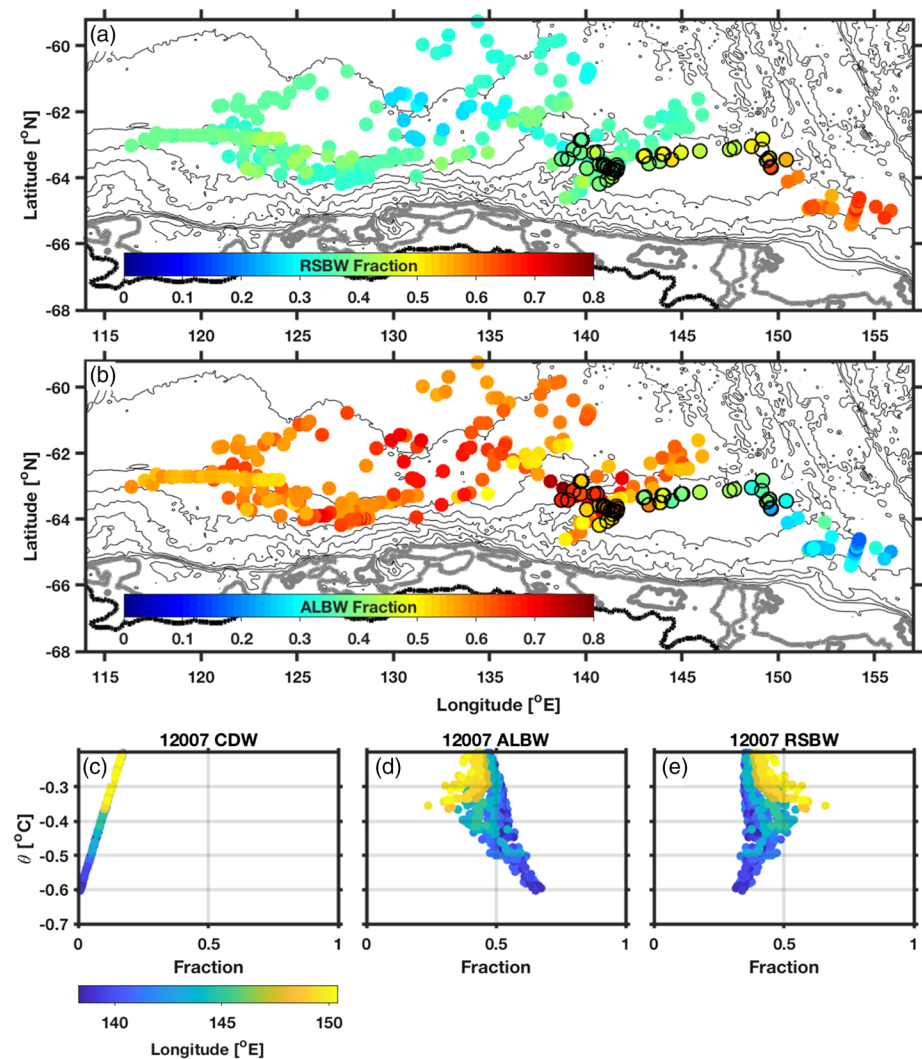
Figure 3. (a) The average fraction (color bar) of new, salty RSBW between the −0.3 and −0.5°C potential isotherms over 500 m bathymetry contours from ETOPO1 with the 0 and 500 m depth isobaths (thick black and gray lines, respectively) emphasized. The profiles of float 12007 are circled in black. (b) Same as (a) but of the average fraction (color bar) of ALBW within 200 m of the bottom, estimated from the ETOPO or the float measured max depth when floats were under ice. (c–e) The results of the OMP analysis for float 12007 are shown, with each profile colored by its longitude to display the zonal gradient (color bar). They depict the distribution of (c) CDW, (d) ALBW, and (e) RSBW against θ in each profile.

denser, colder, and fresher ALBW produced at 142–145°E (Figure 1; AD box). Profiles 19–30 taken in austral fall/winter (May–August) of 2018 of 6042 at 136–138°E (Figure 2c; dark blue) display this higher bottom salinity, but subsequent profiles taken as the float moved westward do not. The zonal gradient in the recent, salty RSBW along the bottom is clearest in these central floats, which show a relationship between longitude and RSBW fraction in the OMP analysis (Figures 3c–3e). The real variation occurs along the −0.4°C isotherm (Figure 3a). From this it is revealed that as the float moved from west to east, it began to record a higher fraction of RSBW at the bottom (Figure 3e).

Farther west still, the influence of recent, salty RSBW is weaker, indicating the greater relative presence of ALBW or older varieties of RSBW in this area. All floats west of 135°E lack the salty kinks or tails that are present in the other floats. In this region, the RSBW fraction is less than 40% along the bottom with slightly higher fractions to the south along the continental slope and lower fractions in the deeper parts of the basin to the north (Figure 3).

Though the results of the simple OMP analysis are reliant on the definitions we prescribed for the endmembers, we found that changing the θ values did not greatly affect the results for our purposes. Changing θ for any endmember by $\pm 0.1°$C caused less than a 6% change in the RSBW fraction found at the bottom of a float profile. However, the fraction of RSBW versus ALBW is much more sensitive to the salinity of the endmembers, which are changing in time (Aoki et al., 2017; Castagno et al., 2019; Jacobs & Giulivi, 2010; Snow et al., 2018). Salinity changes of 0.01 to the ALBW and CDW endmembers result in changes to the bottom RSBW fraction on the order of 5%. The fraction is most sensitive to changes in salinity of the RSBW endmember, for which ± 0.01 results in a change to the fraction on the order of 10%.

4. Discussion

The return of salty RSBW to the AAB in 2018–2020 can be traced with Deep Argo floats. The high salinity bottom water is seen as a salty tail in θ-S curves from float profiles taken in the eastern basin, where RSBW enters the basin and is found at the bottom. It is also seen as a kink in θ-S curves to the west sitting above ALBW (Figure 2c). This can be quantified using a simple OMP analysis, which finds that the bottom water documented by the float profiles furthest to the east had the greatest relative fraction, over 50%, of new RSBW at the bottom compared to only 30% further to the west (Figure 3a). It also finds that the fraction decreases to the west and north across the study region between the $-0.5°$C and $-0.3°$C isotherms (Figure 3a). These θ-S profiles tell the story of dense, new ALBW flowing off the continental shelf and under the lighter and better mixed RSBW coming from the east between 2018–2020 (Figures 2b and 2c). The OMP analysis agrees with this variability along the bottom and displays the signal of a zonal gradient in the amount of ALBW at depth (Figure 3b).

Furthermore, the presence of ALBW here simply identified as waters colder than $-0.5°$C, within Box A (Figure 1) was less than previous hydrographic occupations had observed (Figure 2a). A decrease in the presence of ALBW will lower isotherms, driving warming on isobars. A full analysis of the volume changes and warming of AABW within the basin observed by the floats is outside the scope of this paper but should be a focus of future studies.

Here we quantify the return of a high salinity RSBW to the AAB using the new Deep Argo observational platform. These floats will provide greater spatial and temporal resolution of changes to AABW occurring on seasonal to decadal timescales, allowing the scientific community to better monitor the variability of AABW in this region. While several issues with the float data remain unanswered, including how to determine the location of float profiles taken during winter, all six of the Deep Argo floats deployed in the southern AAB have performed remarkably well despite the harsh conditions. No floats showed salinity drift or were lost during the first two under-ice winters. With more years of data, the temporal and spatial variability in AABW properties within the AAB will be monitored in greater detail. The floats will also serve to bridge the gap between shipboard CTD occupations, allowing for better estimates of variation on longer timescales, such as decadal freshening and warming rates (e.g., Johnson et al., 2019). Outside of the AAB, expansion of the Deep Argo Program past its existing pilot arrays will reveal other changes in the abyssal ocean around the world (Johnson et al., 2015). As Core Argo has drastically advanced our understanding of the upper ocean, Deep Argo is sure to reveal new secrets about the lesser known abyssal waters of the deep ocean.

Data Availability Statement

Argo data were collected and made freely available by the international Argo Program and the national programs that contribute to it (http://www.argo.ucsd.edu, http://argo.jcommops.org). Shipboard repeat hydrographic data were collected and made publicly available by the International Global Ship-based Hydrographic Investigations Program (GO-SHIP; http://www.go-ship.org/, http://cchdo.ucsd.edu). ETOPO1 (https://doi.org/10.7289/V5C8276M) bathymetry data are also made available for the public by the National Center for Environmental Information (NCEI; https://www.ngdc.noaa.gov/mgg/global/).

References

Aoki, S., Kitade, Y., Shimada, K., Ohshima, K. I., Tamura, T., Bajish, C. C., et al. (2013). Widespread freshening in the seasonal ice zone near 140°E off the Adélie/George V Land Coast, Antarctica, from 1994 to 2012. *Journal of Geophysical Research: Oceans*, *118*, 6046–6063. https://doi.org/10.1002/2013JC009009

Aoki, S., Kobayashi, R., Rintoul, S. R., Tamura, T., & Kusahara, K. (2017). Changes in water properties and flow regime on the continental shelf off the Adélie/George V land coast, East Antarctica, after glacier tongue calving. *Journal of Geophysical Research: Oceans*, *122*, 6277–6294. https://doi.org/10.1002/2017JC012925

Aoki, S., Rintoul, S. R., Ushio, S., Watanabe, S., & Bindoff, N. L. (2005). Freshening of the Adélie land bottom water near 140 E. *Geophysical Research Letters*, *32*, L23601. https://doi.org/10.1029/2005GL024246

Bindoff, N. L., Rintoul, S. R., & Massom, R. A. (2000). Bottom water formation and polynyas in Adelie Land, Antarctica. *Papers and Proceedings of the Royal Society of Tasmania*, *133*(3), 51–56. https://doi.org/10.26749/rstpp.133.3.51

Bindoff, N. L., Rosenberg, M., & Warner, M. (2000). On the circulation and water masses over the Antarctic continental slope and rise between 80 and 150°E. *Deep Sea Research Part II: Topical Studies in Oceanography*, *47*(12–13), 2299–2326. https://doi.org/10.1016/S0967-0645(00)00038-2

Boé, J., Hall, A., & Qu, Z. (2009). Deep ocean heat uptake as a major source of spread in transient climate change simulations. *Geophysical Research Letters*, *36*, L22701. https://doi.org/10.1029/2009GL040845

Bryan, F. O., Gent, P. R., & Tomas, R. (2014). Can Southern Ocean eddy effects be parameterized in climate models? *Journal of Climate*, *27*(1), 411–425. https://doi.org/10.1175/jcli-d-12-00759.1

Campagne, P., Crosta, X., Houssais, M., Swingedouw, D., Schmidt, S., Martin, A., et al. (2015). Glacial ice and atmospheric forcing on the Mertz Glacier Polynya over the past 250 years. *Nature Communications*, *6*, 6642. https://doi.org/10.1038/ncomms7642

Castagno, P., Capozzi, V., DiTullio, G. R., Falco, P., Fusco, G., Rintoul, S. R., et al. (2019). Rebound of shelf water salinity in the Ross Sea. *Nature Communications*, *10*, 5441. https://doi.org/10.1038/s41467-019-13083-8

Desbruyères, D. G., Purkey, S. G., McDonagh, E. L., Johnson, G. C., & King, B. A. (2016). Deep and abyssal ocean warming from 35 years of repeat hydrography. *Geophysical Research Letters*, *43*, 10,356–10,365. https://doi.org/10.1002/2016GL070413

Fukasawa, M., Freeland, H., Perkin, R., Watanabe, T., Uchida, H., & Nishina, A. (2004). Bottom water warming in the North Pacific Ocean. *Nature*, *427*, 825–827. https://doi.org/10.1038/nature02337

Ganachaud, A., & Wunsch, C. (2000). Improved estimates of global ocean circulation, heat transport and mixing from hydrographic data. *Nature*, *408*(6811), 453–457. https://doi.org/10.1038/35044048

Gordon, A. L., Bergamasco, A., & Padman, L. (2009). Southern ocean shelf slope exchange. *Deep Sea Research, Part II*, *56*(13–14), 796–817. https://doi.org/10.1016/j.dsr2.2008.10.037

Gordon, A. L., Huber, B. A., & Busecke, J. (2015). Bottom water export from the western Ross Sea, 2007 through 2010. *Geophysical Research Letters*, *42*, 5387–5394. https://doi.org/10.1002/2015GL064457

Gordon, A. L., Zambianchi, E., Orsi, A., Visbeck, M., Giulivi, C. F., Whitworth, T. III, & Spezie, G. (2004). Energetic plumes over the western Ross Sea continental slope. *Geophysical Research Letters*, *31*, L21302. https://doi.org/10.1029/2004GL020785

Jacobs, S. S., & Giulivi, C. F. (2010). Large multidecadal salinity trends near the Pacific–Antarctic continental margin. *Journal of Climate*, *23*(17), 4508–4524. https://doi.org/10.1175/2010JCLI3284.1

Jacobs, S. S., Giulivi, C. F., & Mele, P. A. (2002). Freshening of the Ross Sea during the late 20th century. *Science*, *297*(5580), 386–389. https://doi.org/10.1126/science.1067574

Johnson, G. C. (2008). Quantifying Antarctic bottom water and North Atlantic deep water volumes. *Journal of Geophysical Research*, *113*, C05013. https://doi.org/10.1029/2007JC004477

Johnson, G. C., Lyman, J. M., & Purkey, S. G. (2015). Informing Deep Argo array design using Argo and full-depth hydrographic section data. *Journal of Atmospheric and Oceanic Technology*, *32*(11), 2187–2198. https://doi.org/10.1175/JTECH-D-15-0139.1

Johnson, G. C., Purkey, S. G., Zilberman, N. V., & Roemmich, D. (2019). Deep Argo quantifies bottom water warming rates in the Southwest Pacific Basin. *Geophysical Research Letters*, *46*, 2662–2669. https://doi.org/10.1029/2018GL081685

Joyce, T. M. (1991). Introduction to the collection of expert reports compiled for the WHP programme. WOCE oceanographic programme operations and methods. WOCE operations manual. WHP office report WHPO-91-1, WOCE report no. 68/91. 4 pp. https://www.nodc.noaa.gov/woce/woce_v3/wocedata_1/whp/manuals.htm

Kawano, T., Fukasawa, M., Kouketsu, S., Uchida, H., Doi, T., Kaneko, I., et al. (2006). Bottom water warming along the pathway of lower circumpolar deep water in the Pacific Ocean. *Geophysical Research Letters*, *33*, L23613. https://doi.org/10.1029/2006GL027933

Klatt, O., Boebel, O., & Fahrbach, E. (2007). A profiling float's sense of ice. *Journal of Atmospheric and Oceanic Technology*, *24*(7), 1301–1308. https://doi.org/10.1175/JTECH2026.1

Kobayashi, T. (2018). Rapid volume reduction in Antarctic bottom water off the Adélie/George V land coast observed by deep floats. *Deep-Sea Research Part I*, *140*, 95–117. https://doi.org/10.1016/j.dsr.2018.07.014

Kouketsu, S., Doi, T., Kawano, T., Masuda, S., Sugiura, N., Sasaki, Y., et al. (2011). Deep ocean heat content changes estimated from observation and reanalysis product and their influence on sea level change. *Journal of Geophysical Research*, *116*, C03012. https://doi.org/10.1029/2010JC006464

Lumpkin, R., & Speer, K. (2007). Global ocean meridional overturning. *Journal of Physical Oceanography*, *37*(10), 2550–2562. https://doi.org/10.1175/JPO3130.1

Marsland, S. J., Church, J. A., Bindoff, N. L., & Williams, G. D. (2007). Antarctic coastal polynya response to climate change. *Journal of Geophysical Research*, *112*, C07009. https://doi.org/10.1029/2005JC003291

Massom, R. A., Hill, K. L., Lytle, V. I., Worby, A. P., Paget, M. J., & Allison, I. (2001). Effects of regional fast-ice and iceberg distributions on the behaviour of the Mertz glacier polynya, East Antarctica. *Annals of Glaciology*, *33*, 391–398. https://doi.org/10.3189/172756401781818518

Menezes, V. V., Macdonald, A. M., & Schatzman, C. (2017). Accelerated freshening of Antarctic bottom water over the last decade in the Southern Indian Ocean. *Science Advances*, *3*, e1601426–10. https://doi.org/10.1126/sciadv.1601426

Murphy, D., & Martini, K. (2018). Determination of conductivity cell compressibility for Argo Program CTDs and MicroCATs. 2018 Ocean Sciences Meeting, Portland, OR, Amer. Geophys. Union, IS24E-2622.

Newsom, E. R., Abernathey, R., Bitz, C. M., Bryan, F. O., & Gent, P. R. (2016). Southern Ocean deep circulation and heat uptake in a high-resolution climate model. *Journal of Climate*, *29*(7), 2597–2619. https://doi.org/10.1175/JCLI-D-15-0513.1

Orsi, A. H., Bullister, J. L., & Johnson, G. C. (1999). Circulation, mixing, and production of Antarctic bottom water. *Progress in Oceanography*, *43*(1), 55–109. https://doi.org/10.1016/S0079-6611(99)00004-X

Purkey, S. G., & Johnson, G. C. (2012). Global contraction of Antarctic bottom water between the 1980s and 2000s. *Journal of Climate*, *25*(17), 5830–5844. https://doi.org/10.1175/JCLI-D-11-00612.1

Purkey, S. G., & Johnson, G. C. (2010). Warming of global abyssal and deep Southern Ocean waters between the 1990s and 2000s: Contributions to global heat and sea level rise budgets. *Journal of Climate*, *23*(23), 6336–6351. https://doi.org/10.1175/2010JCLI3682.1

Purkey, S. G., & Johnson, G. C. (2013). Antarctic bottom water warming and freshening: Contributions to sea level rise, ocean freshwater budgets, and global heat gain. *Journal of Climate*, *26*(16), 6105–6122. https://doi.org/10.1175/JCLI-D-12-00834.1

Purkey, S. G., Johnson, G. C., Sloyan, B. M., Smethie, W., Talley, L. D., Wijffels, S., et al. (2019). Unabated bottom water warming and freshening in the South Pacific Ocean. *Journal of Geophysical Research: Oceans*, *124*, 1778–1794. https://doi.org/10.1029/2018JC014775

Rintoul, S. R. (1998). On the origin and influence of Adélie land bottom water. In S. S. Jacobs & R. Weiss (Eds.), *Ocean, ice and atmosphere: Interactions at Antarctic continental margin*, *Antarctic Research Series* (Vol. 75, pp. 151–171). Washington, DC: American Geophysical Union. https://doi.org/10.1029/AR075p0151

Rintoul, S. R. (2007). Rapid freshening of Antarctic bottom water formed in the Indian and Pacific oceans. *Geophysical Research Letters*, *34*, L06606. https://doi.org/10.1029/2006GL028550

Roemmich, D., Alford, A., Claustre, H., Johnson, K., King, B., Moum, J., et al. (2019). On the future of Argo: A global, full-depth, multi-disciplinary array. *Frontiers in Marine Science*, *6*, 439. https://doi.org/10.3389/fmars.2019.00439L124

Roemmich, D., Sherman, J. T., Davis, R. E., Grindley, K., McClune, M., Parker, C. J., et al. (2019). Deep SOLO: A full-depth profiling float for the Argo program. *Journal of Atmospheric and Oceanic Technology*, *36*(10), 1967–1981. https://doi.org/10.1175/JTECH-D-19-0066.1

Shadwick, E. H., Rintoul, S. R., Tilbrook, B., Williams, G. D., Young, N., Fraser, A. D., et al. (2013). Glacier tongue calving reduced dense water formation and enhanced carbon uptake. *Geophysical Research Letters*, *40*, 904–909. https://doi.org/10.1002/grl.50178

Shimada, K., Aoki, S., Ohshima, K. I., & Rintoul, S. R. (2012). Influence of Ross Sea bottom water changes on the warming and freshening of the Antarctic bottom water in the Australian-Antarctic Basin. *Ocean Science*, *8*(6), 2197–2235. https://doi.org/10.5194/osd-8-2197-2011

Silvano, A., Foppert, A., Rintoul, S. R., Haumann, A., Kimura, N., & Macdonald, A. (2020). Recent recovery of Antarctic Bottom Water formation in the Ross Sea driven by climate anomalies. *Nature Geoscience*. https://doi.org/10.1038/s41561-020-00655-3

Sloyan, B. M., & Rintoul, S. R. (2001). Circulation, renewal, and modification of Antarctic mode and intermediate water. *Journal of Physical Oceanography*, *31*(4), 1005–1030. https://doi.org/10.1175/1520-0485(2001)031<1005:CRAMOA>2.0.CO;2

Snow, K., Rintoul, S. R., Sloyan, B. M., & Hogg, A. M. (2018). Change in dense shelf water and Adélie Land bottom water precipitated by iceberg calving. *Geophysical Research Letters*, *45*, 2380–2387. https://doi.org/10.1002/2017GL076195

Swift, J., & Orsi, A. H. (2012). Sixty-four days of hydrography and storms: RVIB Nathaniel B. Palmer's 2011 S04P Cruise. *Oceanography*, *25*(3), 54–55. https://doi.org/10.5670/oceanog.2012.74

Talley, L. D. (2003). Shallow, intermediate, and deep overturning components of the global heat budget. *Journal of Physical Oceanography*, *33*(3), 530–560. https://doi.org/10.1175/1520-0485(2003)033<0530:SIADOC>2.0.CO;2

Talley, L. D., Feely, R. A., Sloyan, B. M., Wanninkhof, R., Baringer, M. O., Bullister, J. L., et al. (2016). Changes in ocean heat, carbon content, and ventilation: A review of the first decade of GO-SHIP global repeat hydrography. *Annual Review of Marine Science*, *8*(1), 185–215. https://doi.org/10.1146/annurev-marine-052915-100829

Tamura, T., Ohshima, K. I., Fraser, A. D., & Williams, G. D. (2016). Sea ice production variability in Antarctic coastal polynyas. *Journal of Geophysical Research: Oceans*, *121*, 2967–2979. https://doi.org/10.1002/2015JC011537

Tomczak, M., & Large, D. (1989). Optimum multiparameter analysis of mixing in the thermocline of the eastern Indian-Ocean. *Journal of Geophysical Research*, *94*(C11), 16,141–16,149. https://doi.org/10.1029/JC094iC11p16141

van Wijk, E. M., & Rintoul, S. R. (2014). Freshening drives contraction of Antarctic bottom water in the Australian Antarctic Basin. *Geophysical Research Letters*, *41*, 1657–1664. https://doi.org/10.1002/2013GL058921

Wendler, G., Stearns, C., Weidner, G., Dargaud, G., & Parish, T. (1997). On the extraordinary katabatic winds of Adélie land. *Journal of Geophysical Research*, *102*(D4), 4463–4474. https://doi.org/10.1029/96JD03438

Williams, G. D., Aoki, S., Jacobs, S. S., Rintoul, S. R., Tamura, T., & Bindoff, N. L. (2010). Antarctic bottom water from the Adélie/George V land coast, East Antarctica (140–149°E). *Journal of Geophysical Research*, *115*, C04027. https://doi.org/10.1029/2009JC005812

Williams, G. D., Bindoff, N. L., Marsland, S. J., & Rintoul, S. R. (2008). Formation and export of dense shelf water from the Adélie depression, East Antarctica. *Journal of Geophysical Research*, *113*, C04039. https://doi.org/10.1029/2007JC004346